

## Electrical Properties of the Ice/Solid Interface

N. N. Khusnatdinov, V. F. Petrenko,\* and C. G. Levey

Thayer School of Engineering, Dartmouth College, Hanover, New Hampshire 03755

Received: October 11, 1996; In Final Form: April 25, 1997<sup>®</sup>

The electrical properties of ice–metal and ice–dielectric (SiO<sub>2</sub>) interfaces were investigated using a field effect transistor technique applied to ice. This technique allows us to measure the initial electric surface charge, the surface conductivity, the mobilities of the charge carriers, and the screening length of the electric charge near the interface. It was found that the surface conductivity depends nonlinearly on the bias applied to the surface and varies from  $1.5 \times 10^{-10} \text{ ohm}^{-1}$  to  $3 \times 10^{-10} \text{ ohm}^{-1}$  as the bias changes between  $\pm 1 \text{ V}$ . Application of a bias voltage irreversibly changes the conductivity and surface charge of ice. The surface charge can be negative or positive within the limits of  $\pm 1 \times 10^{-4} \text{ C/m}^2$ . We measured the mobilities of negative and positive surface charge carriers at a temperature of  $-10^\circ \text{C}$ :  $\mu_- = (3 \pm 0.5) \times 10^{-7} \text{ m}^2/(\text{Vs})$ , and  $\mu_+ = (1.2 \pm 0.3) \times 10^{-7} \text{ m}^2/(\text{Vs})$ . The high mobility of the negative charge carriers indirectly indicates that the molecular structure of ice surface differs from that of the bulk. An upper limit to the estimated screening length of the electrical charge near the ice–metal interface at  $-10^\circ \text{C}$  is 2 nm.

### Introduction

Investigation of electrical properties of the ice–solid interface is very important for fundamental reasons as well as for numerous applications. The adhesion of ice and electrification from friction are examples of phenomena in which the electrical properties of an ice surface in contact with a solid play an important role. A knowledge of the electrical properties can also shed some light on the structure of the ice surface and liquid-like layer (LLL).

The electrical properties of an ice surface can be characterized by such parameters as the work function,  $W_i$ , the surface potential,  $\phi_s$ , the surface charge,  $Q_s$ , the mobility of surface charge carriers,  $\mu$ , and the screening length,  $\lambda$ . To measure these, one can employ the ice particles collision technique,<sup>1</sup> Kelvin's method,<sup>2–6</sup> the Hall effect technique,<sup>7</sup> or electrification from friction.<sup>8,9</sup> The work function is found to be in the range of  $W_i = 4.11 \pm 0.26$  to  $4.3 \text{ eV}$ .<sup>1</sup> The work function of the free ice surface strongly depends on the ambient conditions and can vary by  $\pm 0.2 \text{ V}$ .<sup>2–6</sup> Using the Hall effect, Caranty and Lamfri<sup>7</sup> found an unusually high mobility for the surface charge carriers:  $\mu = 3 \times 10^{-4} \text{ m}^2/(\text{Vs})$ . This is 3 orders of magnitude greater than the mobility of ions in water and ice. Finally, the specific electric charge at the ice surface was found by Petrenko and Colbeck<sup>9</sup> to be  $Q \sim 10^{-4} \text{ C/m}^2$  at  $T = -10^\circ \text{C}$ . In all these experiments ice/(water vapor + air) interfaces have been studied. Even in the friction experiments the surface charge was swept from a free ice surface.

Petrenko and Maeno<sup>10</sup> introduced a new technique in 1987: that of a field effect transistor (FET) applied to ice. Initially, this technique was used to measure the mobilities of negative and positive charge carriers near the ice/solid interface. The mobilities they observed,  $\mu_- = 2.7 \times 10^{-8} \text{ m}^2/(\text{Vs})$ , and  $\mu_+ = 9.2 \times 10^{-8} \text{ m}^2/(\text{Vs})$  at  $T = -33^\circ \text{C}$ , are much lower than those reported by Caranty and Lamfri.<sup>7</sup> Also, a significant change in surface conductivity was reported when applying a bias of  $\pm 1.5 \text{ V}$  normal to the ice surface.

In this paper we further exploit this FET technique applied to ice. We measure the surface charge on the ice–solid

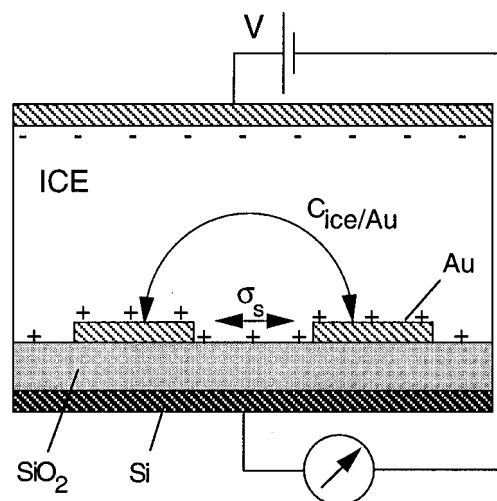


**Figure 1.** Ice field effect transistor. The thickness of the SiO<sub>2</sub> layer is  $L = 1380 \pm 15 \text{ \AA}$ , and the thickness of the silicon wafer is about 0.4 mm. The Au/Ti electrodes cover a surface area of  $S = 1.5 \times 1.5 \text{ cm}^2$ . The thickness of Ti sublayer is  $150 \text{ \AA}$ , and the thickness of the top Au layer is approximately  $600 \text{ \AA}$ . The metal strips are  $50 \text{ }\mu\text{m}$  wide by  $1.5 \text{ cm}$  long, and the distance between the strips is  $50 \text{ }\mu\text{m}$ .

interface, its screening length, and the mobilities of positive and negative charge carriers near the interface.

### Experimental Method

Figure 1 schematically presents the back gated configuration of our ice field effect transistor. An ice sample is placed on an oxidized highly doped silicon wafer (n-type,  $3 \times 10^{-3} \text{ ohm cm}$ ). For simplicity the dimensions of all features are exaggerated. The actual thickness of the thermally grown SiO<sub>2</sub> layer is approximately  $1000 \text{ \AA}$ , and the thickness of the silicon wafer is about 0.4 mm. The metal electrode attached above the ice sample and the Si wafer below are used together to apply a bias normal to the interfaces of ice, SiO<sub>2</sub>, and Si. To measure surface impedance of the ice sample, thin gold interdigitated comb electrodes are used. They are deposited and etched on the SiO<sub>2</sub> layer using a photolithographic technique. For better adhesion two metals were used: titanium, as the first layer, and then gold. The electrodes cover a surface area of  $S = 1.5 \times$

<sup>®</sup> Abstract published in *Advance ACS Abstracts*, July 1, 1997.

1.5 cm<sup>2</sup>. The thickness of Ti sublayer is 150 Å, and the thickness of the top Au layer is approximately 600 Å. The metal strips are 50 μm wide by 1.5 cm long, and the distance between the strips is 50 μm. For simplicity, only two of the 150 strips are shown in Figure 1. The electric charge passed through the system is measured with an electrometer.

The gold comb electrodes are analogous to the source and drain contacts of a FET. The Si wafer and SiO<sub>2</sub> layer are analogous to the gate electrode and gate oxide. The additional upper metal electrode is used to apply a gate bias that is floating with respect to the source and drain. The bias significantly changes the charge distribution at the ice interface. Since the silicon dioxide is a dielectric, essentially all the applied bias,  $V$ , drops across SiO<sub>2</sub> layer. There is, of course, an additional voltage drop on the ice–dielectric interface and ice–metal interfaces due to the contact potentials. The electric field,  $E$ , inside the dielectric layer and at ice surface is  $E = V/d$ , where  $d$  is the thickness of the SiO<sub>2</sub> layer. If we know the capacitance of the SiO<sub>2</sub> layer, then the electric charge,  $Q$ , which sits on ice surface is just  $Q = VC_d$ . The capacitance,  $C_d$ , is estimated from the formula for a plane capacitor with a dielectric constant of silicon dioxide,  $\epsilon = 3.8$ , and is also verified experimentally. The electric field,  $E$ , affects the screening charge and the concentration of charge carriers on ice surface and as a consequence also affects the surface conductivity,  $\sigma_s$ . Both the electric charge on the interface,  $Q$ , and surface conductivity,  $\sigma_s$ , can be measured as functions of the bias applied. Therefore, the mobilities of charge carriers can be estimated. Moreover, by investigating both positive and negative bias conditions, we can determine the mobilities of negative and positive charge carriers. If the surface conductivity is minimum at a particular bias,  $V_{\min}$  (due to depletion of the surface charge), we can estimate the initial surface charge as  $Q_0 = V_{\min}C_d$ .

For a strict analysis, three interfaces need to be considered: ice–SiO<sub>2</sub>, ice–Au comb electrode, and ice–upper electrode. The two latter interfaces are physically similar: both are ice–metal interfaces. There is a slight charge exchange between ice and metal at any voltage applied, even if the voltage is small compared to the ~1.22 eV needed to start electrolysis.<sup>11</sup> Thus, as a bias is applied, we expect no change in the spatial distribution of charge near the ice–metal interface. All charge related to the voltage applied is instead accumulated on the opposite side of Au electrodes, i.e., on the Au–SiO<sub>2</sub> interface. No additional voltage drop will appear on the ice–metal interface.

In case of the ice–SiO<sub>2</sub> interface there is no charge exchange between ice and dielectric, and the spatial distribution of charge at this interface should depend on the external voltage applied.

The following parameters can be measured and determined using the FET technique: (1) The dependence of surface conductivity,  $\sigma_s$ , along the ice–SiO<sub>2</sub> interface on the bias applied between upper electrode and Si wafer can be determined. The initial surface charge,  $Q_0$ , can also be determined from this, as above. (2) The dependence of surface electric charge,  $Q$ , on the bias applied,  $V$ , can be determined. The capacitance is then  $C_d = dQ/dV$ . Combining this with the surface conductivity, we can calculate the mobilities of positive and negative charge carriers on the ice–SiO<sub>2</sub> interface as

$$\mu = \Delta\sigma_s/\Delta Q = \Delta\sigma_s/\Delta VC_d \quad (1)$$

(3) The capacitance between Au electrodes,  $C_{Au}$ , can be measured. Because of the short screening length, the bulk ice acts as an electrode over the gold electrodes, and we can use a parallel plate capacitor approximation. Thus, we can determine the screening length,  $\lambda$ , of the electric charge on ice–Au

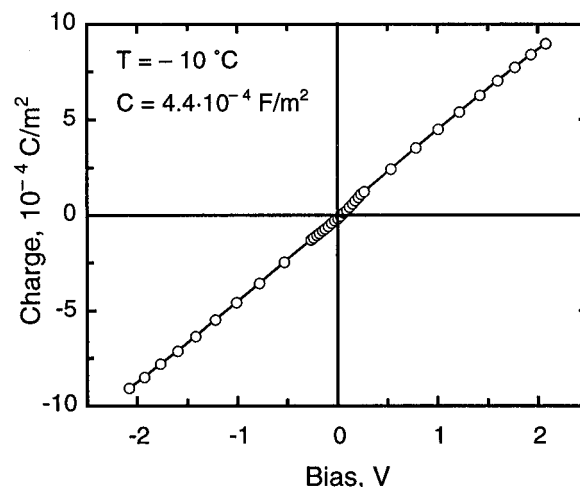


**Figure 2.** Electric charge,  $Q$ , passed through the electrometer and accumulated inside the FET (see Figure 1) is shown as a function of the dc bias applied between the upper electrode and Si wafer,  $T = -10$  °C. From the slope we determine the specific capacitance of the FET to be  $C = 4.4 \times 10^{-4}$  F/m<sup>2</sup>.

electrode:

$$\lambda = \epsilon_0 \epsilon_\infty S / C_{Au} \quad (2)$$

where  $S$  is the flat surface area of the electrodes and  $\epsilon_\infty = 3.2$  is the ice high-frequency dielectric constant, which is appropriate for the screening region.

## Experimental Results and Discussion

Figure 2 shows the electric charge,  $Q$ , passed through the electrometer and accumulated inside FET (see Figure 1) as a function of the bias applied between the upper electrode and Si wafer at  $T = -10$  °C. From the slope of this dependence the specific capacitance of the FET can be estimated as  $C = 4.4 \times 10^{-4}$  F/m<sup>2</sup>. This is the value one would expect for an SiO<sub>2</sub> capacitor of that area. Modeled as series capacitors, the fact that the capacitance of the FET practically coincides with that of SiO<sub>2</sub> layer means that nearly the entire voltage drop is within this dielectric layer. In other words, when  $|V| \geq 0.5$  V, the capacitance of ice–SiO<sub>2</sub> interface is much larger than the capacitance of SiO<sub>2</sub> layer. Thus, the electric field on the ice–dielectric interface is simply determined by the external bias. The  $Q$ – $V$  curve deviates slightly from a linear dependence at small biases (Figure 2). This is because in depletion (low bias) the capacitance of ice–SiO<sub>2</sub> interface is nearly as small as that of the SiO<sub>2</sub> layer.

The surface conductance,  $G_s$ , measured between two comb electrodes increases by about a factor of 3 as the frequency increases from 3 Hz to 30 kHz. Both the bulk and surface conductivity of the ice specimen contribute to these measurements. To separate their contributions, we measured the bulk conductivity of the same specimens using both comb electrodes as one terminal and the stainless steel upper electrode as the second one. Using this result, we estimate that the contribution of the bulk conductivity,  $\sigma_{\text{bulk}}$ , to  $G_s$  is about 500 times smaller than that of the surface conductivity,  $\sigma_s$ , in the frequency range of 3–10 Hz. Thus,  $G_s$  measured at these low frequencies is due to the surface conductivity. As the frequency increases,  $\sigma_{\text{bulk}}$  increases due to Debye dispersion, and above 3 kHz the contributions of  $\sigma_{\text{bulk}}$  and  $\sigma_s$  into  $G_s$  become comparable. For this reason, our measurements of surface conductivity were performed at low frequencies. Figure 3 presents the dependence of the ice–SiO<sub>2</sub> interface surface conductivity,  $\sigma_s$ , measured at

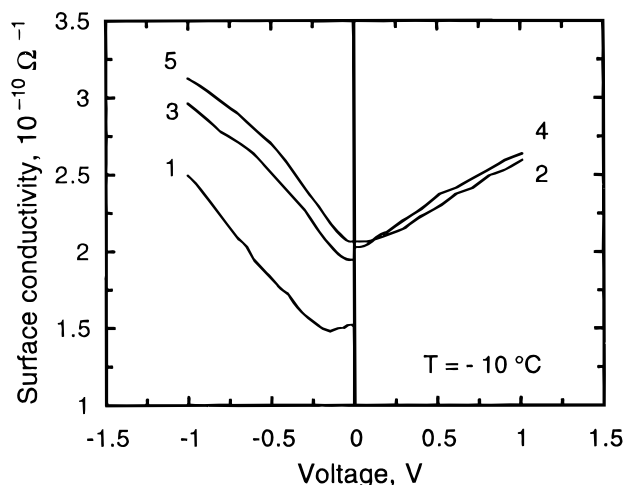


**Figure 3.** Surface conductivity,  $\sigma_s$  ( $f = 10$  Hz), vs dc bias applied between the silicon wafer and the upper electrode,  $T = -10$  °C. Curve 1 corresponds to the initial dependence of the conductivity as the bias increases from 0 to  $-1$  V (the upper electrode is negative). Curves 3–5 present the results of subsequent applications of negative and positive biases.

$f = 10$  Hz, on the bias applied between the silicon wafer and upper electrode at  $T = -10$  °C. Curve 1 corresponds to the initial dependence of the conductivity as the bias increases from 0 to  $-1$  V (the upper electrode is negative). The conductivity reaches a minimum near  $-0.14 \pm 0.01$  V. That means that in this sample there is initial positive surface charge of  $6 \times 10^{-5}$  C/m<sup>2</sup>. This initial surface charge is not reproducible; it can be negative or positive within the limits of  $\pm 1 \times 10^{-4}$  C/m<sup>2</sup>. We suspect that details of the preparation procedure such as internal stress in ice and trace surface contamination and also bias prehistory may affect this charge. When the bias is reduced back to zero, the conductivity does not return to its initial value; however, this residual conductivity decays slightly with time. The subsequent application of a positive bias then changes the surface conductivity as shown by curve 2 of Figure 3. Again, the conductivity after the bias is removed differs from the initial one and slowly decays with time constant of  $123 \pm 8$  s. Curves 3–5 present the result of subsequent applications of negative and positive biases. The minimum of the conductivity shifts to the zero bias region as a result of this bias cycling, and in some tests it shifts slightly into the positive bias region. We can conclude that the application of a bias irreversibly affects the surface conductivity of ice and the stationary charge related to that surface. Second, the slope of the conductivity vs bias curve is larger for negative bias. That means that negative charge carriers are more mobile. The calculated mobilities according to eq 1 are  $\mu_- = (3 \pm 0.5) \times 10^{-7}$  m<sup>2</sup>/(Vs), and  $\mu_+ = (1.2 \pm 0.3) \times 10^{-7}$  m<sup>2</sup>/(Vs).

Let us compare these mobilities with the mobilities of ions and Bjerrum defects in the bulk. The mobilities are:  $9 \times 10^{-8}$ ,  $2.7 \times 10^{-8}$ ,  $<10^{-8}$ , and  $1.8 \times 10^{-8}$  m<sup>2</sup>/(Vs) for H<sub>3</sub>O<sup>+</sup> ions, OH<sup>-</sup> ions, D defects, and L defects, respectively.<sup>11</sup> The analysis depends on the particular model used for the electrical properties of ice surface. Petrenko and Ryzhkin<sup>12</sup> assumed that in a first approximation the subsurface layer structure does not differ from that of the bulk. In this case Jaccard's<sup>13</sup> model can be used for the description of electrical properties of the interface. The calculations show that the differential mobility, defined as  $d\sigma_s/dQ$ , cannot exceed the mobilities of either of one of the charge carriers.<sup>12</sup> Nonetheless, our measurements show that the

differential mobility of the negative charge carriers is higher than all known mobilities. This indicates that at  $T = -10$  °C the structure of ice surface probably differs from that of the bulk. Our measurements indirectly confirm the high values of the mobilities obtained through photoelectromotive force<sup>14</sup> and Hall effect measurements.<sup>7</sup> The 3 orders of magnitude difference between FET and Hall effect mobilities remains to be accounted for.

To estimate the screening length of the surface charge, we have measured the capacitance between the two Au combs,  $C_{Au}$ , using an ac bridge with no dc bias. The capacitance significantly increases as the frequency decreases. This is because of the increased screening of electric field by the slow charge carriers near the electrodes. Even at 3 Hz, the lowest frequency we could reach with our present experimental setup, the capacitance (0.3  $\mu$ F) has not reached its low-frequency (static) value. This gives us an upper limit to the screening length for electric charge near the Au electrode of  $\lambda = 2$  nm at  $T = -10$  °C. The dependence of the screening length,  $l$ , on the perpendicular bias will be investigated in future.

## Conclusions

1. It is found that the surface conductivity depends nonlinearly on the bias applied to the surface and varies significantly as the bias changes. Application of a bias irreversibly changes the conductivity and surface charge of ice.

2. Depending on the bias prehistory and uncontrolled factors during preparation procedure, the surface charge can be negative or positive, within the range of  $\pm 1 \times 10^{-4}$  C/m<sup>2</sup> at  $T = -10$  °C. Interestingly, this variable charge at our ice–solid interface is of the same order as that observed on the free surface of ice using frictional electrification.<sup>9</sup>

3. The mobilities of negative and positive surface charge carriers at  $T = -10$  °C are  $\mu_- = (3 \pm 0.5) \times 10^{-7}$  m<sup>2</sup>/(Vs) and  $\mu_+ = (1.2 \pm 0.3) \times 10^{-7}$  m<sup>2</sup>/(Vs). The high mobility of the negative charge carriers indirectly indicates that the structure of the ice subsurface layer differs from that in the bulk.

4. An upper limit to the screening length of the electric charge near ice–metal interface is  $\lambda = 2$  nm at  $T = -10$  °C.

**Acknowledgment.** This work is supported by NSF under Grant DMR-9413362. It was also supported in part by ARO under Grant DAAH04-95-1-0189 and by ONR under Grant N00014-95-1-0621.

## References and Notes

- (1) Baser, O.; Jaccard, C. (1978), *J. Glaciol.* **1978**, 21, 547.
- (2) Takahashi, T. *J. Atmos. Sci.* **1969**, 26, 1253, 1259.
- (3) Takahashi, T. *J. Atmos. Sci.* **1970**, 27, 453.
- (4) Mazzeda, E.; Del Pennino, U.; Loria, A.; Mantovani, S. *J. Chem. Phys.* **1976**, 64, 1028.
- (5) Caranti, J. M.; Illingworth, A. J. *Nature* **1980**, 284, 44; *J. Phys. Chem.* **1983**, 87, 4078, 4125.
- (6) Caranti, J. M.; Illingworth, A. J.; Marsh, S. J. *J. Geophys. Res.* **1985**, 90, 6041.
- (7) Caranti, J. M.; Lamfri, M. A. *Phys. Lett. A* **1987**, 126, 47.
- (8) Petrenko, V. F. *J. Appl. Phys.* **1994**, 76, 1216.
- (9) Petrenko, V. F.; Colbeck, S. C. *J. Appl. Phys.* **1995**, 77, 4518.
- (10) Petrenko, V. F.; Maeno, N. *J. Phys. C1* **1987**, 48, 115.
- (11) Petrenko, V. F. *Electrical Properties of Ice*, Special Report 93-20; U.S. Army Cold Regions Research and Engineering Laboratory (CRREL): 1994.
- (12) Petrenko, V. F.; Ryzhkin, I. A. *J. Phys. Chem. B* **1997**, 101, 6285.
- (13) Jaccard, C. *Helv. Phys. Acta* **1959**, 32, 89.
- (14) Khusnatdinov, N. N.; Petrenko, V. F. *J. Chem. Phys.* **1994**, 100, 9096.